Measurement and Prediction of Turbo-SIC Receiver Performance for LTE

Sofia Martinez Lopez†, Fabian Diehm‡, Raphael Visoz†, Baozhu Ning†

† Orange Labs, Issy les Moulineaux, France
{sofia.martinezlopez, raphael.visoz, baozhu.ning}@orange.com
‡ Vodafone Chair Mobile Communications Systems, Technische Universität Dresden, Germany
fabian.diehm@ifn.et.tu-dresden.de

***Abstract*—In this contribution, we assess a performance prediction method for turbo successive interference cancellation (turbo-SIC) receivers with the help of lab measurements from a quasi-compliant LTE platform. The presented results show that the calibrated prediction method is able to predict the system performance satisfactorily for the considered modulation and coding scheme.**

***Index Terms*—Turbo-SIC receiver, Interference Cancellation, Performance Prediction, LTE Measurements**

I. Introduction

Within the ongoing global research effort on future wireless communication systems, adaptive allocation of time, code, space and frequency resources based on channel state information at the receiver (CSIR) and users' requirements is widely recognized as a key feature to approach the capacity of MIMO broadband frequency-selective channels. The traditional Radio Resource Management (RRM) and Slow Link Adaptation (LA) have been built on a link-to-system interface, referred to as average value interface [1], in which the individual radio link performance is evaluated through Monte-Carlo simulations averaged over the fast fading statistics. For this approach to be valid the RRM and LA timescales must be large compared to the fast fading dynamics.

On the opposite, current wireless systems evolve toward an enhanced reactivity of RRM and Fast Link Adaptation (FLA) protocols in order to jointly optimize the medium access control and physical layers. Hence, a new type of link-to-system interface, referred to as actual value interface [1], has emerged in which advanced RRM and FLA mechanisms are designed and optimized so as to exploit feedback metrics representative of the instantaneous individual radio link performance, based on performance prediction methods.

In parallel, the success of turbo codes [2] has inspired new potentially capacity achieving coded modulations and, through the so-called turbo principle [3], revolutionized reception theory. New spatial multiplexing architectures and non-orthogonal multiple-access techniques based on powerful coding schemes have been proposed to achieve very high spectral efficiency, whose relevance is, however, conditional upon iterative processing at the receiver.

The research presented in this paper has received funding from the European Commissions' Seventh Framework Programme FP7-ICT-2009 under the grant agreement no 247223 also referred to as ARTIST4G.

These two trends, namely, Cross Layer optimization and turbo processing, call for the development of new physical layer abstractions that can capture the iterative receiver performance (per iteration and per user) conditional on the CSIR. This has been recently investigated in the framework of the EU funded project ARTIST 4G for the class of iterative Minimum-Mean-Square-Error Interference Cancellation (MMSE-IC) joint decoding receivers or turbo Successive Interference Cancellation (turbo-SIC) receivers (as they are referred to by 3GPP). This class of receivers is known to be particularly interesting in terms of its trade-off between performance and complexity and is seen as a promising candidate for LTE-Advanced. The proposed prediction methods are described in [4] and [5] for perfect and imperfect CSIR, respectively. In this paper, we assume that the number of pilot symbols is sufficient to ensure close to perfect Channel Estimation (CE) and therefore use the prediction method described in [4] based on the symbol-wise Mutual Information Effective SNR Mapping (MIESM) technique [6].

As of now, the validation of the proposed prediction method has relied on simulations with Rayleigh fading channel models. The main goal of this paper is to show the validity of the proposed prediction method [4] for actual recorded channels encountered in experimental setups. Here, we stick to a given simple Modulation and Coding Scheme (MCS) based on a rate 1/2 turbo code and QPSK modulation. Indeed, the prediction method was shown to be very accurate for MCSs based on convolutional code of the same rate and modulation and Rayleigh fading MIMO channel models. Since our main interest in this paper is the relative discrepancy between the predicted and the experimental performance (not the absolute performance), we consider the de-mapper together with the two recursive systematic convolutional codes of the turbo code as a black box characterized by two Look Up Tables (LUTs) as in the case of convolutional codes.

The paper is organized as follows. In Sections II and III we present the model of the interference cancellation receiver and the prediction method, respectively. We then describe the conducted measurements in Section IV, before we present the results in Section V. Finally, the paper is concluded in Section VI.

978-1-4673-1881-5/12/$31.00 ©2012 IEEE

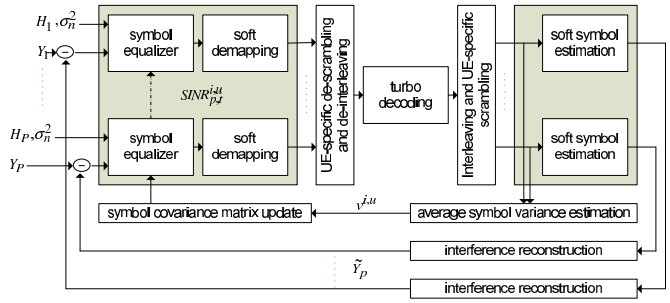

Fig. 1. Receiver model at iteration i, user u

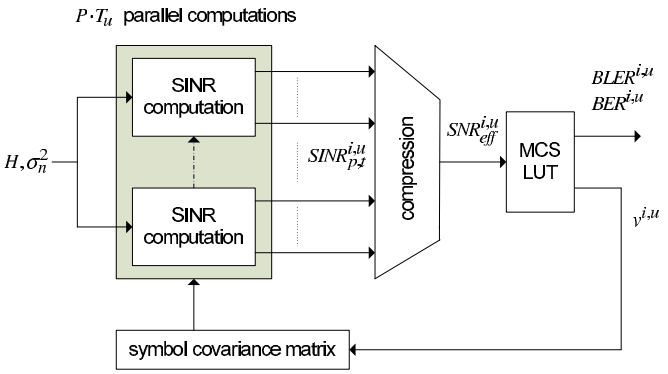

Fig. 2. Prediction method at iteration i, user u

II. Receiver Model

Fig. 1 depicts a schematic of the turbo-SIC receiver that successively exchanges soft probabilistic information between the de-mapper and the decoder. We consider the uplink direction in which multiple users transmit data to the base station on the same radio resources. Within each iteration the users are treated in a serial way. The cancellation order is not optimized. P is the number of block fading states that are experienced during the transmission of a codeword. For each channel state p, $\hat{H}_p$ (matrix of dimension $R \times T$) is the estimate of the channel, where R is the number of receive antennas and T is the total number of transmit antennas. T_u is the number of transmit antennas of user u. Assuming Space Time Bit-Interleaved Coded Modulation (BICM), the users code over P channel uses (e.g., subcarriers/OFDM symbols) and over T_u spatial dimensions. Thus, at the receiver, there are PT_u parallel MMSE equalizing stages before the filtered symbols of user u are passed to the de-mapper. Note that extrinsic information of previous iterations is not useful at the de-mapper since Gray labeling is used (see [1] for other labelings). The output of the de-mapper is de-scrambled and de-interleaved before it is handed to the soft-in soft-out turbo decoder. For the results presented in this paper, we carry out one iteration within the turbo decoder for each iteration of the interference cancellation without loss of generality. The Log A-Posteriori Probability Ratios (LAPPRS) computed by the turbo-code both on systematic and parity bits are considered after re-interleaving as a Log A priori Probability Ratios (LAPRs) on bits for interference reconstruction. It is important to stress that the use of LAPPRs rather than Log Extrinsic Probability Ratios (LEXTPRs) is in complete violation of the turbo principle [7]. Still, it was witnessed as beneficial in terms of performance [7]. Assuming independence between bits [4, Assumption A1], the aforementioned LAPRs are used to compute the a priori probability mass functions (pmfs) of the transmitted symbols for every user, antenna, and time indexes (k), i.e., $\left\{P(s_{p,t,k}^{u,i}) = s, \forall s \in A\right\}$. This is an approximation as the bits are not completely independent due to the fact that the used LAPRs contain the channel observation. Each transmit symbol is then reconstructed by its Mean Square Error (MSE) estimate conditional on the symbol pmfs which is simply the mean of the transmitted symbol. This reconstruction is then used to subtract the received interference for the next interference cancellation stage. The pmfs are also used to compute the average symbol variance v that is taken into account to adjust the Linear Minimum Mean Square Error filters (LMMSE) of the next user. This variance v ($0 < v < 1$) decreases as the reliability of the interference reconstruction increases.

The reader is referred to [4] for more detailed information about the used receiver. A comparison between different receivers for LTE can be found in [8] and in [9].

III. Prediction Method

The prediction method used in this paper has been established in [4] and relies on MIESM technique at symbol level. Fig. 2 depicts the prediction of user u at iteration i. The first step is the computation of the PT_u SINRs at the output of the MMSE receive filters. In the second step, the different SINRs are compressed using MIESM to yield the effective SNR. In other words, the SINRs are transformed into the mutual information domain according to the used modulation alphabet, where they are averaged before being transformed back to yield the effective SNR. In the third step a pre-computed LUT is used that characterizes the receiver performance for AWGN channels, for the chosen MCS. The output of the LUT is the expected receiver performance at the given effective SNR in terms of BER or BLER and the value of the average symbol variance $v^{i,u}$ described in section II. In the next iteration, this value is used to update the symbol covariance matrix that is taken into account when computing the PT_u SINRs at the output of the filters.

IV. Measurement Setup

To test the described prediction algorithm, a small scenario was selected for the lab measurements. In this scenario, two single-antenna UEs transmit on the same time and frequency resources to one base station that is equipped with two receive antennas. Thus, $T_1 = T_2 = 1$ and $R = 2$.

The used test equipment for the performed measurements has basic compliance with LTE Release 8. Unlike LTE, the system however employs OFDMA in the uplink direction instead of SC-FDMA. The main OFDM parameters and frame parameters are given in Table I. For each measurement the UEs were placed randomly in the lab room (about 8m x 6m) and transmitted using the same modulation and coding scheme.

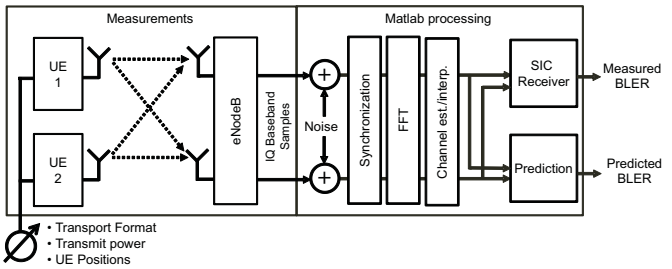

Fig. 3. Measurement setup and basic blocks of the evaluation chain

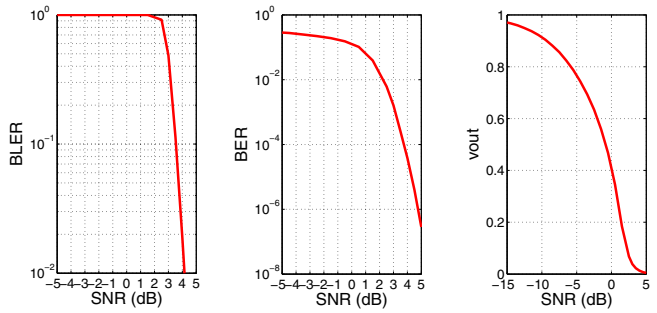

Fig. 4. Look Up Tables for the prediction method, based on measured data

Fig. 3 depicts the main measurement and evaluation procedure. At the eNodeB, the baseband samples from the measurements are stored on a hard drive and then processed using Matlab. Since the transmit conditions in the small lab environment are very favorable (very high SNRs), the measured BLER tends to be zero. Thus, to observe a wider range of SNR values we added artificial noise (AWGN) to the received samples as a first step in the processing chain.

TABLE I
TRANSMISSION PARAMETERS

Parameter	Value
Bandwidth mode	20 MHz
FFT size	2048
Available subcarriers	1200
Sampling rate	30.72 MHz
Subcarrier spacing	15 kHz
Transmit Time Interval (TTI)	1 ms
OFDM symbols/TTI	14
Subcarriers per Physical Resource Block (PRB)	12
Used PRBs for transmission	10
Occupied bandwidth	1.8 MHz
Modulation scheme	QPSK
Code rate	1/2
Data OFDM symbols per PRB	11
Resource elements used per code block ($= P$)	1540
T_u	1
R	2

As depicted in Fig. 3, the next processing step is the timing synchronization. In this step, the FFT window is optimized based on the correlation with the cyclic prefix over the incoming baseband samples. After the FFT, the channel is estimated. To allow CE, the transmit frames are organized as follows: every 4th and 11th OFDM symbol in each TTI are occupied by reference symbols. These symbols (that are made up of Zadoff-Chu sequences) are spread over two consecutive subcarriers for each terminal with an orthogonal spreading sequence that allows separating the pilots from the individual UEs at the receiver. The channels on the remaining resource elements of each Physical Resource Block (PRB) are finally estimated using linear interpolation between the pilot positions.

To obtain a comparison between measured and predicted results, the channel estimates and an estimate of the noise floor (measured on unused subcarriers) are passed to the prediction algorithm. At the same time, these inputs are forwarded to the receiver algorithm together with the received data blocks to obtain the measured bit error rates.

The required LUTs for the prediction method were obtained by SISO AWGN measurements using a cable connection between transmitter and receiver as well as variable attenuators (Fig. 4).

V. RESULTS

The analysis is divided into three parts. First, the measured pilots and payload are processed and the resulting receiver performance is compared to the prediction results, as explained above. Then we show the impact of CE error and the various hardware impairments (e.g., residual carrier frequency offsets and power amplifier non-linearity) on the accuracy of the prediction method. Finally, we present an improvement in the prediction method that reduces the gap between the measured and predicted BER.

A. Imperfect channel estimation, hardware impairments

The results for the measurements are depicted in Fig. 5. The plotted BERs each correspond to the measured BER at one measurement location with one variance of noise. The x-axis denotes the effective SNR that is computed during the prediction algorithm (Fig.2), based on the estimated channels and the noise floor. The predicted BER for the same effective SNR can be seen on the black reference curve. Thus, the closer the circles approach the reference curve, the more accurate the prediction works.

As the measurements were conducted in a static environment, the observed channels did not change for one measurement location. In order to improve the accuracy, the recorded TTIs were evaluated multiple times (with additional random noise as explained before) until 100 wrong code blocks were observed. As it is impossible to remove the noise included in the measurements, the noise in the receiver processing is not completely independent, which slightly reduces the accuracy of the BER for high SNR values.

For the sake of readability, we focus on the cases where the BER of user one at iteration one is above 10^{-3}, so that successive iterations can still achieve a noticeable enhancement. More than 1000 BER measurements are depicted in each plot of Figs 5-7.

In Fig. 5, the points corresponding to the first iteration of the first user are on both sides of the reference curve, meaning the receiver performance is sometimes better and sometimes worse than expected. However, from the first interference subtraction onwards, most of the points lie above the prediction curve. Therefore, we can either state that the assumption of close to

perfect CE is not valid in our setting or that the prediction itself is too optimistic. Both statements are correct, as shown in the next subsection.

B. Perfect channel estimation, no hardware impairments

In order to assess the impact of the CE errors and the hardware impairments (e.g., carrier frequency offset, and amplifier non-linearity), we carried out simulations using the measured channels and enforcing the underlying prediction assumption of perfect CE. To achieve this, instead of processing the measured payload symbols, the measured channels where used together with simulated transmit signals X to generate the received signals $Y = \hat{H} \cdot X + n$, where $\hat{H}$ is the measured channel matrix, and n is Gaussian noise.

The BERs obtained for this case (perfect CE) are depicted in Fig. 6. Comparing it to Fig.5, we observe that the accuracy increases. As explained before, the used prediction [4] can only account for limited channel uncertainty (close to perfect CE assumption). As explained in section IV, the CE procedure used in the test platform is not LTE compliant. In fact, the orthogonality of the pilot signals is impaired by frequency selectivity and residual carrier frequency offsets, leading to less accurate CE. Thus, part of the mismatch between measured BER and predicted BER in Fig. 5 originates from imperfect channel knowledge. Still, Fig. 6 also reveals that the prediction is too optimistic even though perfect CSIR is now made available. This observation was less visible in the case of convolutional codes and is MCS dependent.

C. Improvement of the prediction method

Since the underlying assumption of independence between bits [4, Assumption A1] used by the prediction method is not strictly valid, the predicted performance is likely to be too optimistic as shown in Figs. 5 and 6 (this would even not be true for an infinite-length interleaver, due to the use of LAPPRS for interference reconstruction as stated before). To increase the prediction accuracy, we weighted the variance $v^{i,u}$ by a calibration factor $\beta > 1$, i.e., $v^{i,u} = \max(1, \beta v^{i,u})$. Exhaustive simulations showed that this calibration factor depends on the MCS and does not vary significantly with respect to the channel time and frequency selectivity nor the number of transmit and receive antennas.

Using exhaustive search, we observed the best fit for $\beta = 2.5$. Fig. 7 shows that the match between the BER based on recorded channels (with perfect CE) and the predicted BER with $\beta = 2.5$ is now very good. This validates the calibrated prediction method for turbo codes and the considered MCS. Note that, comparing Fig. 7 with Fig. 6, the effective SNRs are different since they depend on the value of β (except for iteration 1, user 1). As a result, the circles of Fig.6 are shifted to the left in Fig. 7, fitting better to the prediction. Interestingly, the proposed calibration method nicely improves the prediction accuracy by reducing the variance of the error between predicted and simulated BER.

VI. Conclusion

In this paper we presented measurement results to validate a performance prediction method for MIMO Turbo-SIC receivers using turbo-codes. It was the first time that the prediction method was tested using measured radio channels. For this purpose, indoor measurements were carried out using a test platform with basic compliance to LTE Release 8. In the validation scenario, 2 UEs transmit to an eNodeB on the same transmission resources. More than one thousand BER measurements were obtained and compared to the prediction. The mismatch between the predicted BER and the measured BER can be explained by two main reasons. The first reason is that the assumption of close to perfect CE does not hold for the used test platform. The second reason is the optimistic behavior that the prediction method exhibits even with perfect CSIR. To counteract this impairment, we proposed a simple calibration procedure. It is shown to significantly increase the prediction accuracy and it demonstrates that the calibrated prediction method is a good candidate for enabling fast link adaptation in real system with turbo-SIC receivers provided that the CE is sufficiently good. In future work, the presented observations could be extended to imperfect CSIR by predicting the average BLER conditional on a channel estimate as proposed in [5].

Acknowledgements

The authors would like to thank Ainoa Navarro Caldevilla from TU Dresden for her significant support with the measurements and their preparations.

References

[1] S. Hämäläinen, P. Slanina, M. Hartman, A. Lappeteläinen, and H. Holma, "A novel interface between link and system level simulations," Proc. ACTS Mobile Telecommunications Summit'97, Aalborg, Denmark, pp. 599-604, Oct. 1997.

[2] C. Berrou, A. Glavieux, and P. Thitimajshima, "Near Shannon limit error-correcting coding and decoding," in Proc. IEEE ICC'93, Geneva, Switzerland, pp. 1064-1070, May 1993.

[3] J. Hagenauer, "The turbo principle: Tutorial introduction and state of the art," in Proc. 1st International Symposium on Turbo Codes, Brest, France, pp. 1-12, Sept. 1997.

[4] R.Visoz, A.Berthet and M.Lalam, "Semi-analytical performance prediction methods for iterative MMSE-IC multiuser MIMO joint decoding" IEEE Trans. on Commun., vol. 58, No. 9, pp. 2576-2589, Sep. 2010.

[5] B. Ning, R. Visoz, A.O. Berthet, "Semi-analytical performance prediction method for iterative MMSE-IC detection and semi-blind channel estimation," in Proc. IEEE VTC'11 Spring, Hungrary, Budapest, May 2011.

[6] K.Brueninghaus, D. Astely, T. Sälzer, S. Visuri, A. Alexiou, S. Karger, and G. A. Seraji, "Link performance models for system level simulations of broadband radio access systems," in Proc. IEEE PIMRC'05, vol. 4, Berlin, Germany, pp.2306-2311, Sept. 2005.

[7] M. Witzke, S. Baro, F. Schreckenbach, and J. Hagenauer, "Iterative detection of MIMO signals wih linear detectors," in Proc. Annual Asilomar Conference on Signals, Systems, and Computers, California, USA, Nov. 2002.

[8] J.Ketonen, M.Juntti, J.R. Cavallaro, "Performance-complexity comparison of receivers for a LTE MIMO-OFDM system", IEEE Trans. On Signal Process., vol.58, No. 6, pp.3360-3372, Jun. 2010.

[9] C.S. Park, Y.-P.E Wang, G. Jöngren, D. Hammarwall, "Evolution of uplink MIMO for LTE-Advanced," IEEE Commun. Mag., vol.49, No. 2, pp.112-121, Feb. 2011.

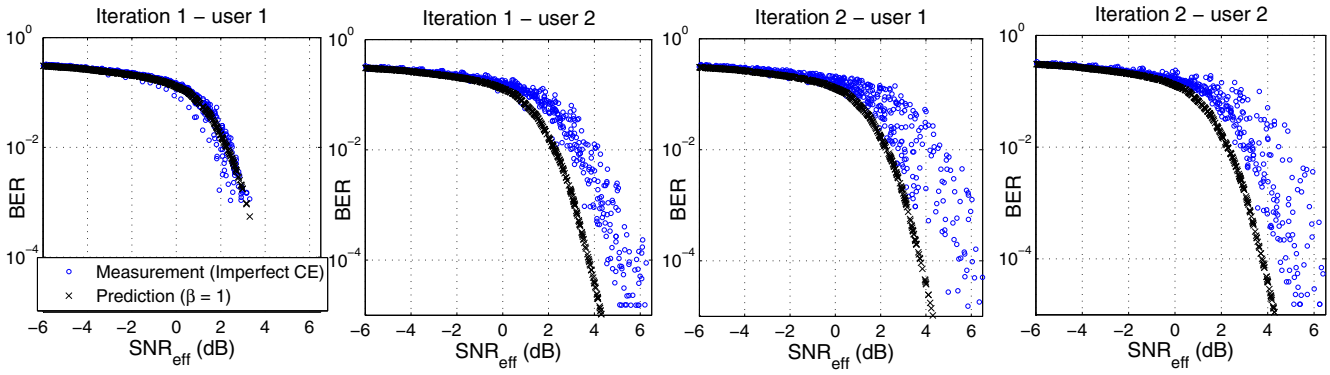

Fig. 5. BER based on measurements (Imperfect CE) versus prediction

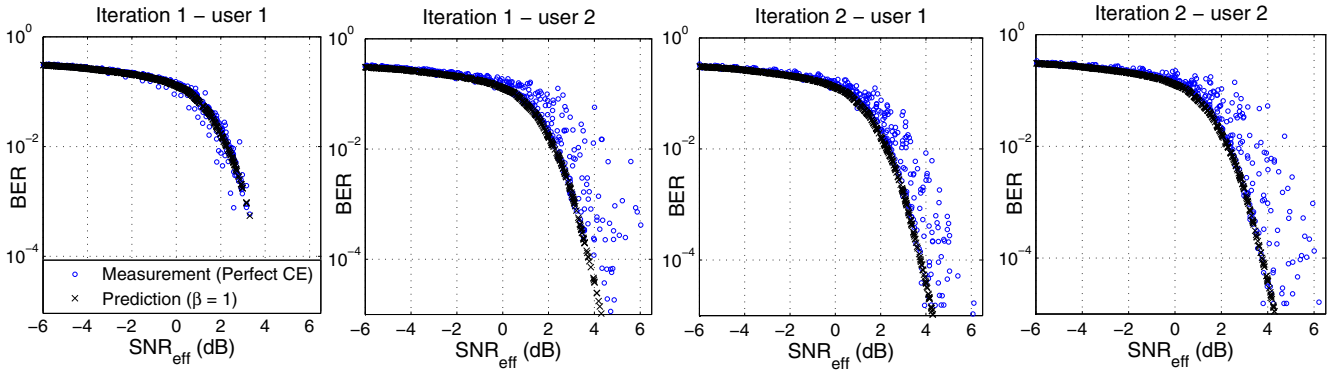

Fig. 6. BER based on measurements (Perfect CE) versus prediction

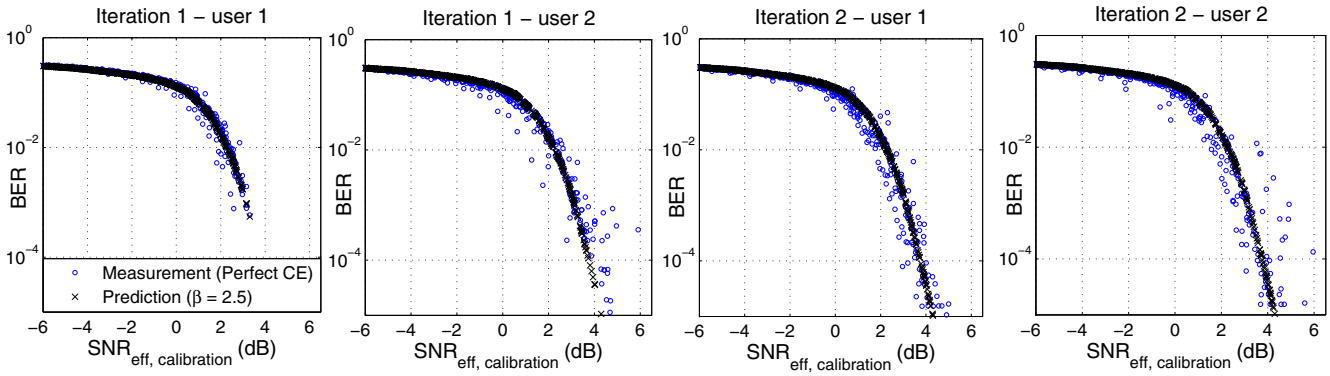

Fig. 7. BER based on measurements (Perfect CE) versus calibrated prediction